Meteorological drought projections for Australia from downscaled high-resolution CMIP6 climate simulations

Rohan Eccles[1], Ralph Trancoso[1,2], Jozef Syktus[2], Sarah Chapman[1], Nathan Toombs[1], Hong Zhang[1], Shaoxiu Ma[1], Ryan McGloin[1]

[1]Climate Projections and Services, Department of Energy and Climate, Queensland Government, Brisbane, Australia
[2]School of The Environment, The University of Queensland, Brisbane, Australia

Correspondence to: Rohan Eccles (rohan.eccles@gmail.com)

Abstract. Climate change is projected to lead to changes in rainfall patterns, which, when coupled with increasing evapotranspiration, has the potential to exacerbate future droughts. This study investigates the impacts of climate change on meteorological droughts in Australia using downscaled high-resolution CMIP6 climate models under three Shared Socioeconomic Pathway (SSP) scenarios. The Standardised Precipitation Index (SPI) and the Standardised Precipitation Evapotranspiration Index (SPEI) were used to assess changes to the frequency, duration, percent time, and spatial extent of droughts. There were consistent increases in droughts projected for south-west Western Australia, southern Victoria, southern South Australia, and western Tasmania using SPI and SPEI. There were significantly larger increases for SPEI derived droughts, with consistent increases projected for most of the country. The largest increases occurred at the end of the century and under the high emissions scenario (SSP370), demonstrating the influence of emissions on extreme droughts. For instance, if emissions reached high levels by the end of the century, the area subject to extreme drought in drought prone Southern Australia would be 2.8 greater than if they were kept to low levels using SPI, and 4 times greater if assessed using SPEI. The insights generated from these results and supplementary tailored datasets for Australian Local Government Areas and River Basins are essential to better inform decision making and future adaptation strategies at national, regional, and local scales.

1 Introduction

Droughts are among the costliest climate hazards in the world, with significant ramifications for agriculture, society, and the

25 environment (Cook et al., 2018). Between 1998 and 2017, droughts were estimated to have cost $2.3 trillion dollars (USD), affecting 1.5 billion people globally (United Nations, 2018). Notable recent major drought events have occurred in California (He et al., 2017), the Mediterranean (Kelley et al., 2015), and in Australia (Van Dijk et al., 2013). The recent Australian Millenium drought which lasted from 2001 to 2009 (Van Dijk et al., 2013) was estimated to have cost as much as 1.6 % of the nation's gross domestic product (Horridge et al., 2005). Compared to other countries of similar population, Australia is

30 disproportionately impacted by drought; ranked 5th for economic impacts of droughts and 15th for the number of people affected between 1990 and 2014 (González Tánago et al., 2016). A number of studies have highlighted the importance of droughts in Australia, with consequences for a range of other factors including bushfires (Devanand et al., 2024), agriculture (Xiang et al., 2023), water supply (Maier et al., 2013), dust storms (Leys et al., 2023), and public health (Johnston et al., 2011).

In comparison to other natural hazards, determining the onset and severity of a drought event is complex since they are

35 characterised by a gradual build-up, where the largest impacts typically only emerge after many months or years (Kiem et al., 2016). The definition of drought varies according to its application, but can generally be split into meteorological, hydrological, and agricultural droughts (Zargar et al., 2011). Meteorological droughts relate to prolonged deficits in rainfall but may be exacerbated through high temperatures and evaporation, hydrological droughts describe impacts on streamflow and other water systems (e.g., reservoirs or lakes) (Van Dijk et al., 2013), while agricultural drought primarily focus on soil moisture content

40 (Zargar et al., 2011).

Droughts are usually monitored and assessed through indicators and indices (Svoboda and Fuchs, 2016). Two of the most commonly applied indices for meteorological droughts are the Standardised Precipitation Index (SPI; McKee et al., 1993) and the Standardised Precipitation Evapotranspiration Index (SPEI; Vicente-Serrano et al., 2010). SPI is a rainfall-based index derived from accumulated monthly rainfall values and can be used to describe droughts at a range of timescales and across

45 different locations. When assessed at shorter timescales (~3 months), SPI has been shown to relate closely to soil moisture and agricultural droughts, while at longer timescales SPI (>12 months) it is more closely related to hydrological droughts (e.g., reservoirs and streams) (Zargar et al., 2011). SPEI is an extension of SPI, calculated as the difference between precipitation and potential evapotranspiration (P − PET), and as such better reflects changes to the overall water deficit by considering the impacts of both the atmospheric supply and evaporative demand on the water budget. SPEI has also been shown to be more

50 closely related to agricultural impacts than SPI (Labudová et al., 2017; Xiang et al., 2023). The main advantage of the SPI and SPEI over other drought indices is that they provide multi-scalar results that are directly comparable across different regions and climate zones (e.g., arid vs humid regions).

Under climate change, there is potential for more frequent and severe drought events as a result of temperature increases and changed precipitation patterns, particularly in already drought prone regions (Huang et al., 2016; Zhao and Dai, 2015). Several

55 studies have evaluated the impacts of climate change on droughts using Global Climate Models (GCMs), which have pointed

towards increased drought risk over the 21st century for many regions, including Australia (Cook et al., 2018, 2020; IPCC, 2023; Spinoni et al., 2020). These studies are, however, based on GCMs with coarse resolutions (~200 km), which have difficulty representing precipitation patterns over complex terrain (Reder et al., 2020) and as such, are not always suitable to provide reliable information to support adaptation and mitigation policy as well as decision-making at regional scales.

60 Additionally, some studies have been reliant on a limited number of climate models, which can have large inter-model and metric-dependent discrepancies leading to uncertain results (Ukkola et al., 2018). There is therefore a need to consider multiple climate simulations as well as high-resolution models to account for inter-model uncertainties while simulating regional climate granularity.

In order to better represent small-scale features and processes, Regional Climate Models (RCMs) have been employed for

65 drought projection studies across different regions (Gao et al., 2017; Secci et al., 2021; Spinoni et al., 2018), including for regions within Australia (Herold et al., 2021; Syktus et al., 2020). RCMs have been shown to have improved skill in representing patterns of local precipitation and the impacts of topography, coasts, and land-use changes compared to GCMs (Boé and Terray, 2014; Chapman et al., 2023; Grose et al., 2019; Tian et al., 2013). These models (GCMs and RCMs) are the best physically-based approaches currently available to understand future drought processes, characteristics and impacts.

70 Several studies have considered the impacts of climate change on droughts across Australia (Kirono et al., 2011, 2020; Kirono and Kent, 2011; Mpelasoka et al., 2008) or within a sub-section of the continent (Feng et al., 2019; Herold et al., 2021; Shi et al., 2020). Mpelasoka et al. (2008) estimated that soil-moisture based drought frequency would increase by 20-40% over most of Australia by the 2030s compared to 1975-2004. Similar increases in drought extent were projected for most regions by (Kirono et al., 2011; Kirono and Kent, 2011). More recently, Kirono et al. (2020) applied SPI and Standardised Soil Moisture

75 Index (SSMI) to calculate projected future droughts using an ensemble of 37 raw Coupled Model Intercomparison Project (CMIP5) GCMs. They projected significant increases to drought hazard metrics, except for frequency, with greater increases for the SSMI compared to SPI. Herold et al. (2021) used SPI derived from 3 months of accumulated rainfall to investigate changes to 1-in-20-year drought events across southeast Australia with an ensemble of four RCMs. They projected these events would occur approximately 1-in-5 years by the end of the century for large parts of southeast Australia. These studies have,

80 however, relied on projections derived from CMIP5 or earlier. A number of studies have evaluated how future droughts are projected to change based on the latest CMIP6 GCMs (Cook et al., 2020; Wang et al., 2021; Zeng et al., 2022; Zhao and Dai, 2022), which point to increased meteorological droughts for much of Australia (Ukkola et al., 2020; Vicente-Serrano et al., 2022) despite the uncertainties in precipitation (Trancoso et al., 2024). However, research to date has largely focussed on applying coarse GCM outputs to assess future droughts, which are not appropriate to infer drought-related processes at regional

85 scales, especially in a drought prone country such as Australia.

This study expands on the available body of knowledge for future meteorological droughts in Australia, employing an ensemble of 60 CMIP6 high-resolution simulations (15 historical and 45 future simulations) dynamically downscaled as part of the Queensland Future Climate Science Program (QFCSP) to a 10 km resolution over the whole of Australia (Chapman et

al., 2023). These projections form part of a national strategy for climate projections and underpin Queensland's climate services

90   and adaptation planning. The objectives of this contribution are:

      i)   to assess changes in future projected meteorological droughts, including the frequency of occurrence, duration, spatial extent, and percent time in drought estimated using SPI and SPEI;

      ii)   to compare changes in droughts between three different emissions pathways, two categories of drought severity, and two drought indices;

95   iii)   to evaluate how different climatic regions of the Australian continent are projected to experience future droughts under three different emissions pathways and estimate the time of emergence for significant shifts to occur.

2 Methodology

2.1 Study Area

100   This study evaluated changes to drought indices for the entire Australian continent, which encompasses a range of climate regions, including equatorial, tropical, sub-tropical, temperate, Mediterranean, and arid regions. We assess drought changes to four Natural Resource Management (NRM) super-clusters for Australia, namely; Eastern Australia, Northern Australia, Rangeland, and Southern Australia, which are grouped based on a combination of climate and biophysical factors and have been widely adopted within Australia (Grose et al., 2020; Kirono et al., 2020) for assessing the impacts of climate change (Fig.

105   1).
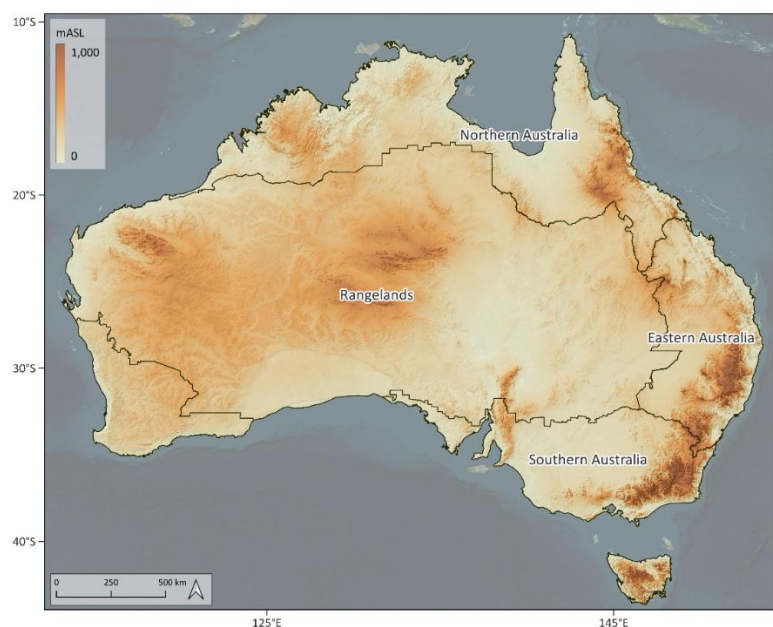
Figure 1: Extent of study area and sub regions adopted in this study showing NRM super-clusters for the whole of Australia with elevation derived from SRTM (Shuttle Radar Topography Mission) in metres above sea level (mASL).

110

2.2 Data

We used an ensemble of 60 downscaled climate model simulations derived from 11 different CMIP6 GCMs (Table 1), some model variants were downscaled multiple times. The ensemble consists of 15 runs for historical simulations and three sets of 15 runs for future simulations under three Shared Socioeconomic Pathways (SSP126, SSP245 and SSP370), representing low,

115 moderate, and high-emissions pathways, respectively. The ensemble of GCMs used in this study was selected in order to best represent the future spread in the climate change signal from the ensemble of global CMIP6 models, while prioritising models which were better able to represent the Australian climate (Trancoso et al., 2023). Dynamic downscaling was performed for the full ensemble of GCMs using the Conformal Cubic Atmospheric Model (CCAM; Scientific description - CCAM.) developed by CSIRO (McGregor and Dix, 2008). CCAM was run using a stretched C288 grid, which consists of a model

120 resolution of approximately 10 km for Australia. A downscaling approach outlined by Hoffman et al. (2016) was applied for this purpose, which involved correcting for modelled biases in sea surface temperatures and sea ice. This approach has been found to improve the simulations of climate from CCAM and other regional climate models (Hoffmann et al., 2016; Kim et al., 2020; Lim et al., 2019). Five of the CCAM simulations were run using dynamic atmosphere-ocean coupling as presented in Table 1. The downscaling approach adopted was shown to significantly improve the performance over the host GCMs for

125 precipitation and temperature in all seasons, with the largest improvements noted for climate extremes (Chapman et al., 2023). We used observational data to evaluate the SPI and SPEI indices during the historical period (1980 – 2010). Daily gridded precipitation data with a spatial resolution of 0.05° (approximately 5 km) were obtained from the Australian Gridded Climate Data Project (AGCD; Evans et al., 2020). While daily gridded (resolution of 0.05°) PET data derived from the Penmen Monteith reference crop equation was obtained from the Australian Water Outlook. All observational data was re-gridded to

130 the same grid resolution as the downscaled climate projections using distance weighting interpolation for precipitation and bilinear interpolation for PET.

135

140

Table 1. Details of the 15 climate model simulations downscaled from 11 CMIP6 GCMs considered in this study.

CMIP6 Model	Model full name	Resolution	Ensemble member	CCAM setup
ACCESS-ESM1.5	Australian Community Climate and Earth System Simulator, version 1.5	1.875 x 1.25°	r6i1p1f1 r20i1p1f1 r40i1p1f1	atmospheric atm-ocean coupled atm-ocean coupled
ACCESS_CM2	Australian Community Climate and Earth System Simulator, version 2	1.875 x 1.25°	r2i1p1f1	atm-ocean coupled
CMCC-ESM2	Centro Euro-Mediterraneo sui Cambiamenti Climatici	0.9 x 1.25°	r1i1p1f1	atmospheric
CNRM-CM6-1-HR	Centre National de Recherches Météorologiques Coupled Global Climate Model, version 6.1, high-resolution	0.5 x 0.5°	r1i1p1f2 r1i1p1f2	atmospheric atm-ocean coupled
EC-Earth3	European Community Earth-System Model, version 3	0.8 x 0.8°	r1i1p1f1	atmospheric
FGOALS-g3	Flexible Global Ocean-Atmosphere-Land System Model, grid point version 3	2.5 x 2.5	r4i1p1f1	atmospheric
GFDL-ESM4	Geophysical Fluid Dynamics Laboratory Earth System Model, version 4	1 x 1°	r1i1p1f1	atmospheric
GISS-E2-2-G	Goddard Institute for Space Studies Model E2.2G	2. x 2.5°	r2i1p1f2	atmospheric
MPI-ESM1-2-LR	Max Planck Institute Earth System Model, version 1.2, low resolution	1.9 x 1.9	r9i1p1f1	atmospheric
MRI-ESM2-0	Meteorological Research Institute Earth System Model, version 2.0	1.125 x 1.125°	r1i1p1f1	atmospheric
NorESM2-MM	Norwegian Earth System Model, version 2, 1 degree resolution	1 x 1°	r1i1p1f1 r1i1p1f1	atmospheric atm-ocean coupled

145   2.3 Drought Indices

We used the SPI and SPEI indices to assess changes to future meteorological droughts based on downscaled climate simulations. SPI reflects changes to precipitation only, while SPEI is calculated from the difference between precipitation and

PET and therefore reflects changes to the overall water deficit by considering the impacts of increased temperatures and evaporative demand in addition to atmospheric water supply. To calculate SPEI, we apply PET derived from the Penman-

150 Monteith reference crop method (Allen et al., 1998), which is a physically-based approach. This was calculated offline using daily CCAM outputs of solar radiation, vapour pressure, maximum and minimum temperature, mean sea level pressure, and wind speed.

PET and precipitation data were aggregated to monthly totals for all grid cells and used to calculate SPI and SPEI with the SPEI R Package (Beguería et al., 2017). For SPI, we fitted precipitation data to the gamma distribution, while for SPEI we

155 fitted the difference between precipitation and PET to the log-logistic distribution as recommended by Vicente-Serrano et al. (2010). Normality tests were performed using the Shapiro-Wilk test at the 95% confidence level on the derived SPI and SPEI to ensure the grid cells conformed to normality. Most grid cells (over 85%) conformed to normality for all months (Fig. S1 in the supplementary materials). As the outputs follow a normal distribution, different categories of drought and also wetness may be classified according to the calculated SPI/SPEI Z-value. Table 2 shows the adopted classification scheme used for both

160 SPI and SPEI as suggested by McKee et al. (1993).

Table 2. SPI and SPEI drought classification table following McKee et al. (1993) with associated probability of event from the chosen calibration period

SPI/SPEI values	Categories	Probability of event
SPI/SPEI ≤ -2	Extreme drought	2.3%
-2.0 < SPI/SPEI ≤ -1.5	Severe drought	4.4%
-1.5 < SPI/SPEI ≤ -1.0	Moderate drought	9.2%
-1.0 < SPI/SPEI < 1.0	Near normal	68.2%
1.0 ≤ SPI/SPEI < 1.5	Moderate wet	9.2%
1.5 ≤ SPI/SPEI < 2.0	Severe wet	4.4%
SPI/SPEI ≥ 2.0	Extreme wet	2.3%

165 A variety of different accumulation periods may be applied when calculating the SPI/SPEI, ranging from 1 to 48 months. Smaller accumulation periods (1 to 3 months) can be used to assess impacts on systems that are quick to respond to droughts (e.g., soil moisture and small creek flows), while longer accumulation periods (12 to 48 months) better reflect the impacts to slower-responding systems to water deficits, such as groundwater and reservoir levels. We adopted a 12-month accumulation period for our assessments of SPI and SPEI as this was considered as a suitable timeframe for water deficits to impact various

170 hydrological and agricultural systems (Zargar et al., 2011).

When assessing droughts using historical data, the full period of historical data available is generally used to fit the distribution, with the World Meteorological Organisation recommending a minimum of 30 years (Svoboda et al., 2012). However, when assessing changes to these indices as a result of climate change, a historic calibration period is commonly adopted to fit the distribution. The derived transfer function from the calibration period is then applied to estimate the SPI and SPEI for the

175 future period, allowing for a comparison of projected future dryness and wetness compared to the recent past. For our assessment, we have adopted a calibration period from 1981-2010 to fit the distribution, which was used to calculate SPI and SPEI over the full timeseries, containing both historical and future simulations (1981-2100).

The SPI and SPEI timeseries results are calculated at the grid-cell scale for the observational data and for the ensemble of downscaled climate simulations and are used to detect the occurrence of droughts. For the sake of validation, projected

180 droughts from historical simulations were compared against those estimated from observational data. A drought event is defined when the SPI or SPEI falls below a value of -1 and finishes once the value exceeds -1 again. The definitions for the categories of drought severity are presented in Table 2. In this study, we focus on the changes to all droughts (moderate, severe, and extreme) and to extreme droughts. Metrics relating to the frequency, duration, spatial extent, and percent time in drought were calculated for each of the drought categories. Here, the frequency is defined as the total number of events recorded over

185 a given time period, the duration is the average duration of recorded drought events (in months), the percent time in drought is the fraction of time droughts occur, and the spatial extent is the percent of a region in drought. We evaluated the biases in the drought metrics from each of the climate models considered compared to the observational data over the period used to fit the distributions (1981-2010).

2.4 Climate Change Assessment

190 We assessed the impacts of climate change on droughts for the 2050s (2041-2060) and the 2090s (2081-2100) relative to the 1995-2014 reference period, which is in line with the IPCC assessment. The historical simulations were used to benchmark the reference period while future simulations were used to quantify the climate change impacts. Results from each of the 45 future simulations were evaluated individually and in a weighted model ensemble, which adopted a one model one vote rule. This weights the models according to the number of downscaled simulations per host model (i.e., the three ACCESS-ESM1-

195 5 models were averaged to a single model, while the two NorESM2-MM and CNRM-CM6-1-HR were also averaged), resulting in an 11-model average. Results in this paper are assessed across the four NRM super cluster regions (Fig. 1). Additional supplementary datasets tailoring projected drought impacts to Australian Local Government Areas and River Basins are also made available (Eccles, 2024).

We evaluated timeseries results for the individual models and the ensemble average. For this purpose, a 20-year moving

200 average was applied to determine long-term changes to SPI and SPEI values and to remove year-to-year variability. Outputs of both SPI and SPEI follow a normal distribution, with defined probabilities of occurrence for the different drought categories in the calibration period (Table 2). We therefore assessed when significant changes to the long-term average values occurred based on a 10% and 20% shift to the probability. A 10% shift towards dryness corresponded to the 40th percentile of SPI and SPEI results from the calibration period, while a 20% shift corresponded to the 30th percentile. The goal of this analysis was

205 to determine the time of emergence for significant shifts in the long-term climate to take place and to compare the results across regions and emissions scenarios. We also evaluated changes to the probability density function (PDF) of the SPI and

SPEI to determine changes to the distribution of the different drought events. This was further applied to assess the changes to the percentage of area under drought for the four NRM super-clusters assessed.

3 Results

3.1 Validation of Projected Droughts

We compared differences between CCAM derived metrics of droughts and those derived from observational products for the calibration period (1981-2010) to quantify the biases of the historical simulations. The metrics derived from historical simulations for individual model runs tended to over-estimate SPI-based metrics and underestimate SPEI-based metrics, when compared against observational data (Fig. 2). The variability of biases across individual model runs was expected as heterogeneous runs from host GCM models were selected to estimate future model uncertainty. However, biases to the ensemble average were substantially reduced, denoting a good match to the observational data, particularly for SPEI.
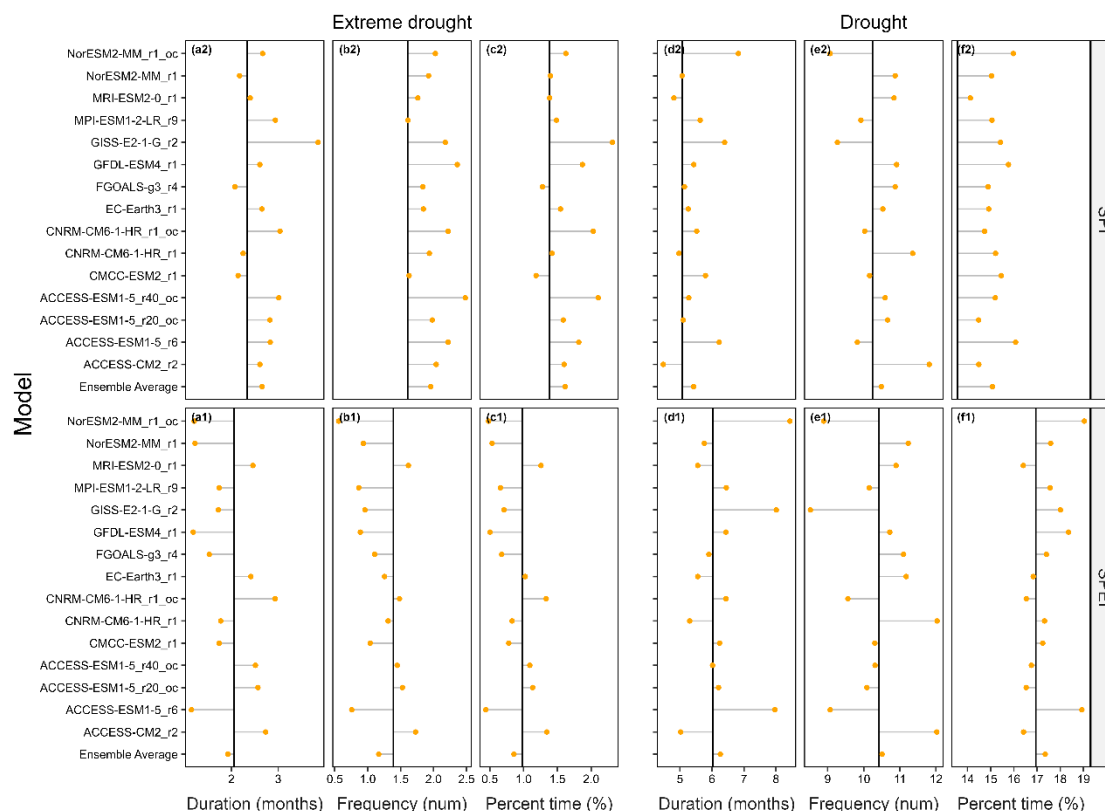
Figure 2: Comparison of the differences in calculated metrics of drought and extreme droughts between climate model simulations and observations for the calibration period over all of Australia (1981 to 2010). Drought metrics from observation data are presented as solid black lines, while points show metrics from climate model simulations.

3.2 Climate Change Assessment

3.2.1 Changes to SPI and SPEI

The 20-year moving average SPI and SPEI time-series results under SSP370 are presented in Fig. 3. Decreases to SPEI were
225   observed for all the models across all regions, indicating substantial agreement on future drying using SPEI. The largest
decreases were observed by the end of the century. By contrast, the results for SPI were more heterogeneous, with many
models predicting increases and decreases, as evident by the spread of models in the direction of trend (Fig. 3), though the
ensemble averages tended towards a slight increase in wetness for the Rangelands and an increase in dryness for Southern
Australia. These same patterns of change can be noted in the raw timeseries results of the ensemble averages presented in the
230   supplementary materials for each emissions scenario (Fig. S2 to Fig. S4).

The time taken for the ensemble average to reach a 10% and 20% shift of the probability towards dryer conditions (according
to the Z-score) are shown by vertical dashed lines. These thresholds were not reached for SPI using the ensemble average
(though they are for some individual models) and hence no vertical dashed lines are shown. For SPEI a 10% shift towards
drier conditions was reached by 2040 for the Rangelands and Southern Australia, and a 20% shift by 2060. These shifts of 10
235   and 20% were delayed in Northern Australia and Eastern Australia to approximately 2060 and 2090, respectively. Results for
SSP126 and SSP245 are available in the supplementary materials (Fig. S5 and Fig. S6).
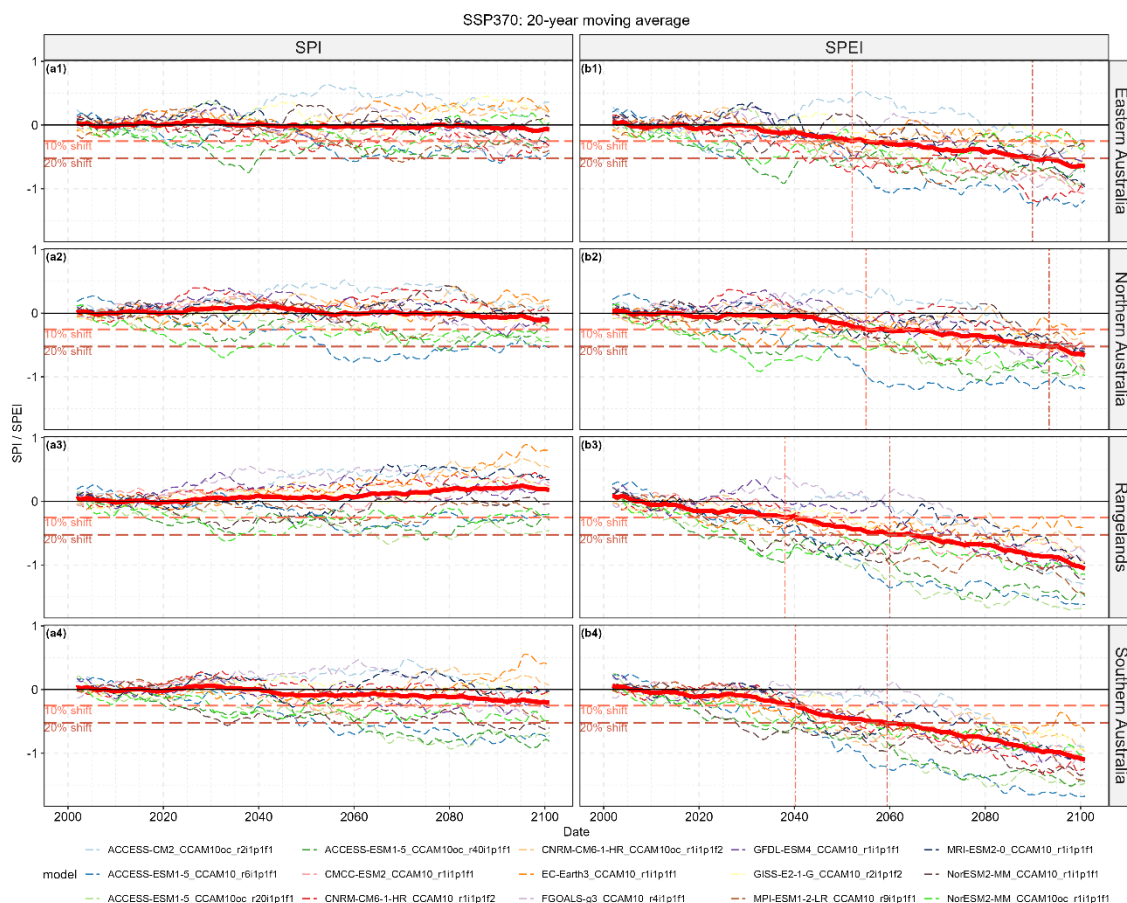
Figure 3: Timeseries results for SPI and SPEI calculated as a 20-year moving average for each climate model considered with the ensemble average shown in red for each of the regions under the SSP370 scenario. Dotted lines show the time taken for the ensemble average value to shift by 10% and 20% (according to the Z-score).

More wetting was evident under the high emissions scenario for the Rangelands compared to the low or moderate scenarios when considering only precipitation using SPI, but more drying when the additional impacts of increased PET were considered through SPEI (Fig. 4). For SPEI, all emissions scenarios consistently predict a 10% shift in the moving average value by approximately 2040, and a 20% shift by approximately 2060. Only at the end of the century, were there significant differences in SPEI between the different emissions scenarios, with the greatest decreases noted under SSP370. Similar patterns were also observed for the other NRM super-clusters assessed (Fig. S7 to Fig. S9).
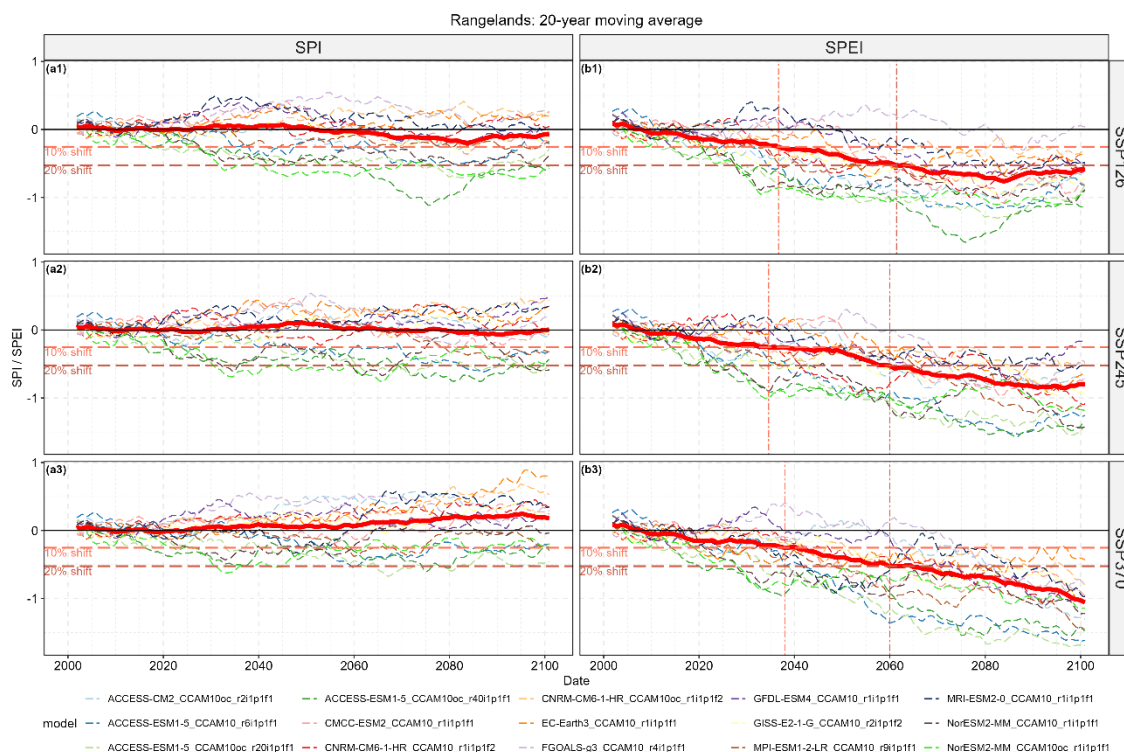
Figure 4: Timeseries results for SPI and SPEI calculated as a 20-year moving average for each climate model considered with the ensemble average shown in red for each of the emissions scenarios for the Rangelands. Dotted lines show the time taken for the ensemble average value to shift by 10% and 20% (according to the Z-score).

There was a notable shift towards more pronounced drought conditions in the 2050s and 2090s compared to the reference period (1995-2014) when assessing the probability density function (PDF) of both SPI (Fig. 5) and SPEI (Fig. 6). Relatively minor changes to the PDF were noted for SPI in Eastern Australia and Northern Australia, though there was a tendency towards lower SPI values (increased dryness) by the 2050s and 2090s compared to the reference period (1995-2014). Decreases were more pronounced for Southern Australia, while the changes to the Rangelands appeared minimal. In all regions, the largest changes were noted for the negative tails of the SPI distribution (< -1), indicating an increased likelihood of more pronounced periods of moderate to extreme droughts. Interestingly, in most regions, this appears to have come at the cost of the near normal and moderate wet categories (-1 to 1.5) but does not look to have changed the positive tail of the distribution (> 1.5) to the same extent. A quantification of the change to the probability of occurrence for the different categories of events under SSP370 confirms that the increase in extreme and severe droughts primarily led to decreased near normal and moderately wet conditions (Table 3). The probability of extreme wetness is shown to have also increased in all regions using SPI. This suggests an overall shift towards more periods of drought, while maintaining similar levels or increased periods of pronounced wetness (Fig. 5). There was an overall shift away from typical climate conditions towards more periods of both extreme drought and wetness (Table 3).

When the additional impacts of increased evaporation are considered using SPEI, there were notable shifts towards dryer
270   conditions in all regions, especially by the end of the century (Fig. 6). This was particularly true for the Rangelands and
Southern Australia (Table 3), which are subject to low rainfalls and therefore more strongly influenced by relative increases
to PET. The shifts towards lower SPEI values and dryer conditions were seen across the full distribution of data, including the
tails suggesting a future decrease to periods of wetness which was not reflected in the SPI results. Though only minor changes
were projected for extreme wetness under SSP370 (Table 3). changes are shown to be considerably smaller under the moderate
275   and low emissions scenarios (Table S1 and S2).
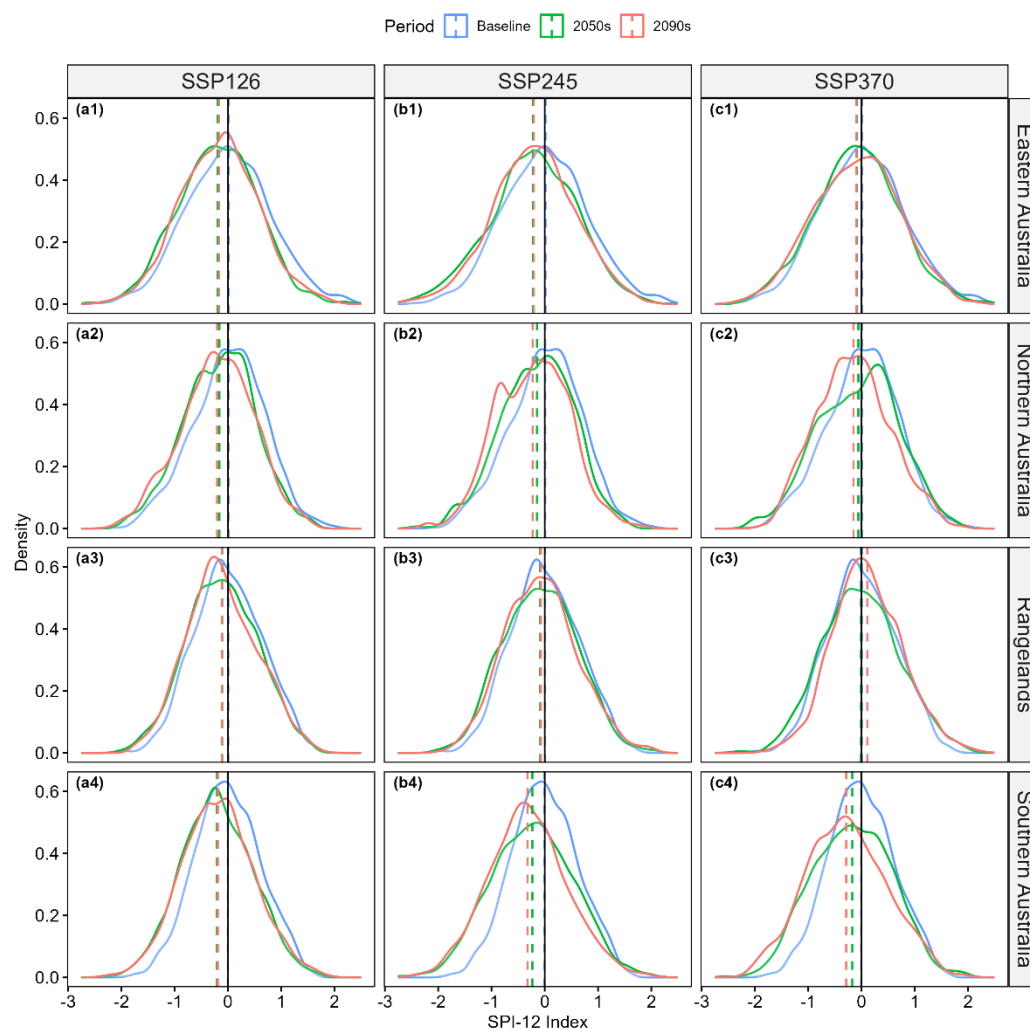
**Figure 5: Probability density function plot of SPI values from the full ensemble of climate models for the reference period (1995-
2014), 2050s (2041-2060), and 2090s (2081-2100). Results are shown for the three SSPs in the four NRM super-clusters considered.**
280   **Dotted lines show mean values.**
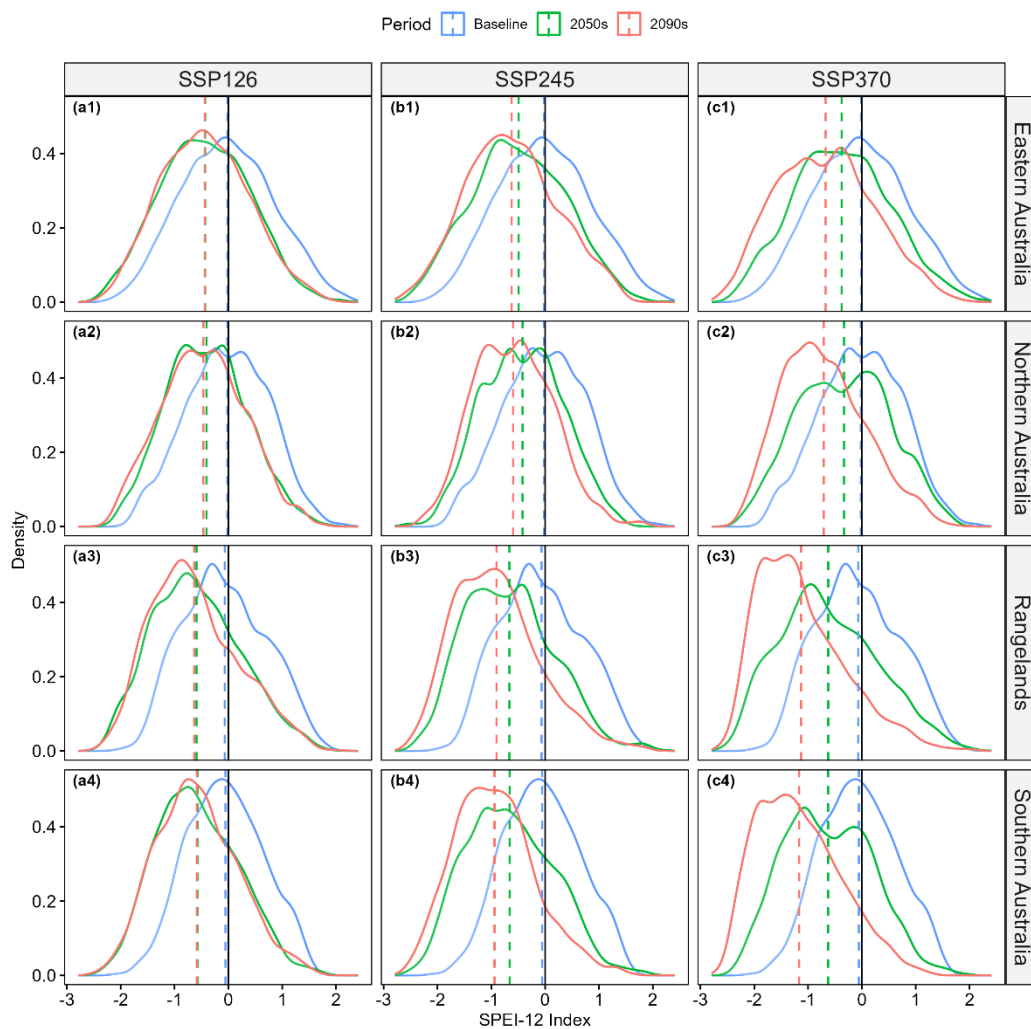
Figure 6: Probability density function plot of SPEI values from the full ensemble of climate models for the reference period (1995-2014), 2050s (2041-2060), and 2090s (2081-2100). Results are shown for the three SSPs in the four NRM super-clusters considered. Dotted lines show mean values.

Table 3. Projected absolute percent change to the percent of time spent in different drought and wetness categories by the 2050s and 2090s compared to the reference period (1995-2014) using the ensemble average under SSP370. Red colours denote larger increases, while green colours denote decreases.

Index	Category	Eastern Australia		Northern Australia		Rangelands		Southern Australia	
		2050s	2090s	2050s	2090s	2050s	2090s	2050s	2090s
SPI	Extreme drought	0.75	1.41	1.37	1.52	0.68	-0.26	2.93	5.74
	Severe drought	0.48	1.49	1.22	1.35	0.46	-0.78	2.07	2.98
	Moderate drought	0.08	1.22	0.59	1.71	-0.15	-1.82	1.42	1.84
	Near normal	0.01	-3.84	-4.36	-3.38	-3.76	-2.39	-7.33	-11.37
	Moderate wetness	-1.13	-1.1	-0.61	-1.63	-0.13	1	-0.88	-1.46
	Severe wetness	-0.49	-0.08	0.35	-0.46	0.7	1.41	-0.02	0.1
	Extreme wetness	0.3	0.9	1.43	0.89	2.2	2.84	1.81	2.17
SPEI	Extreme drought	3.7	9.88	4.29	8.23	8.71	20.99	8.88	24.78
	Severe drought	3.05	7.81	4.06	8.8	6.4	10.73	6.6	9.67
	Moderate drought	2.66	5.29	1.91	6.26	2.9	3.57	3.66	2.55
	Near normal	-4.08	-14.6	-7.39	-14.71	-12.97	-26.23	-13.71	-27.98
	Moderate wetness	-3.13	-5.13	-2.43	-5.55	-3.88	-6.68	-4.02	-6.52
	Severe wetness	-2.23	-3.27	-1.1	-2.96	-1.99	-3.49	-2.29	-3.75
	Extreme wetness	-0.13	-0.43	0.56	-0.32	0.55	-0.43	0.56	-0.36

290

3.2.2 Changes to Drought Extent

A notable increase in the area affected by droughts was projected for all regions under SSP370 considering SPEI, with the largest increases noted by the end of the century and for Southern Australia and the Rangelands (Fig. 7). This same increase in drought extent, however, was not seen for SPI except in Southern Australia, where there was a trend towards more extreme droughts, though the magnitude of the change was significantly smaller than that seen for SPEI. Interestingly, the largest increases to drought extent occurred for extreme and severe events, while the extent of moderate droughts which are a more common occurrence under present conditions, did not increase significantly for either SPI or SPEI. These results suggest that the largest increases to droughts will occur for extreme events, rather than moderate events (Fig. 7 and Table 3). This is especially true when the impacts of increased PET are considered using SPEI. The results for SSP245 and SSP126 show more modest increases to drought extents for all the NRM super-clusters (Fig. S7 and Fig. S8), especially for the area in extreme drought, though the pattern of change remains the same.

PDFs of the area affected by extreme droughts are presented for SPI (Fig. 8) and SPEI (Fig. 9). For SPI, an increase to the area affected by extreme droughts can be seen in all regions and emissions scenarios, except for in the Rangelands under SSP370, where a minor decrease was projected by the end of the century (Fig. 8). These increases are typically in the order of 1 to 2%

305 of the area, representing a near doubling of the total area affected by extreme droughts. The increase was especially significant in Southern Australia, where the average extent of extreme drought increases from 1.9% in the reference period to between 4.3 and 5.0% by the 2050s and 4.0 and 7.8% by the 2090s, depending on the emission scenario adopted. Under the high emissions scenario, this represented a fourfold increase to the area under extreme droughts. The magnitude of the changes were even more pronounced for SPEI, changing from 1.6% in the reference period to between 8.8 and 10.6% by the 2050s and

310 8.1 and 27.9% by the 2090s, depending on the emission scenario adopted (Fig. 9).
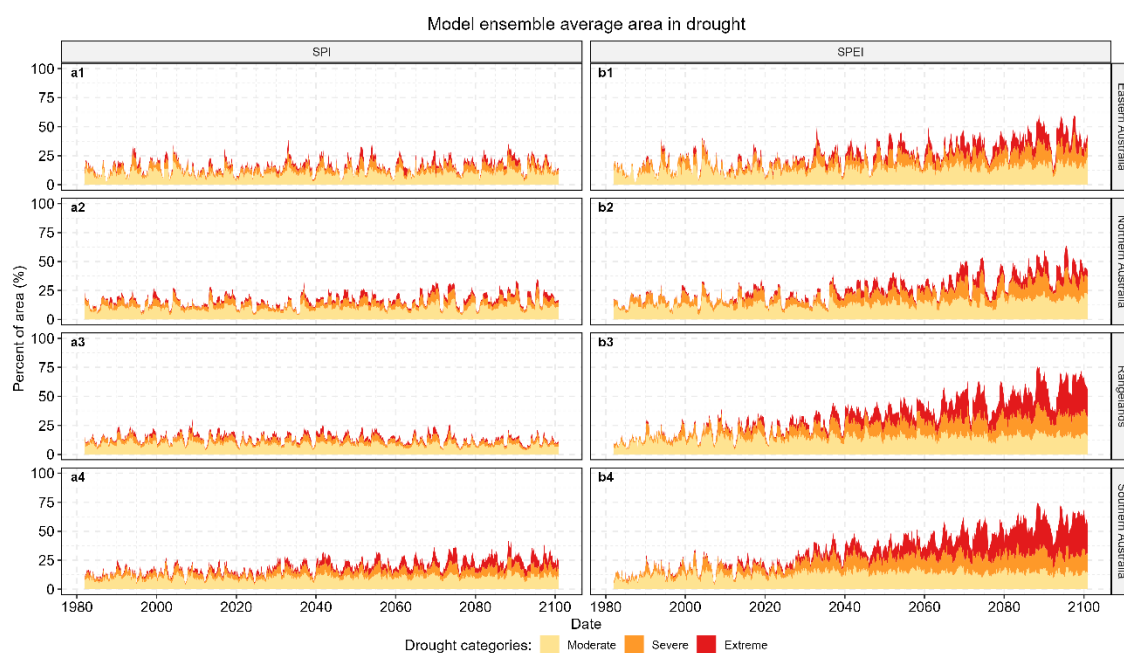
Figure 7: Timeseries of the ensemble average percent of area in drought in the four NRM super-clusters for SPI and SPEI under ssp370.

315
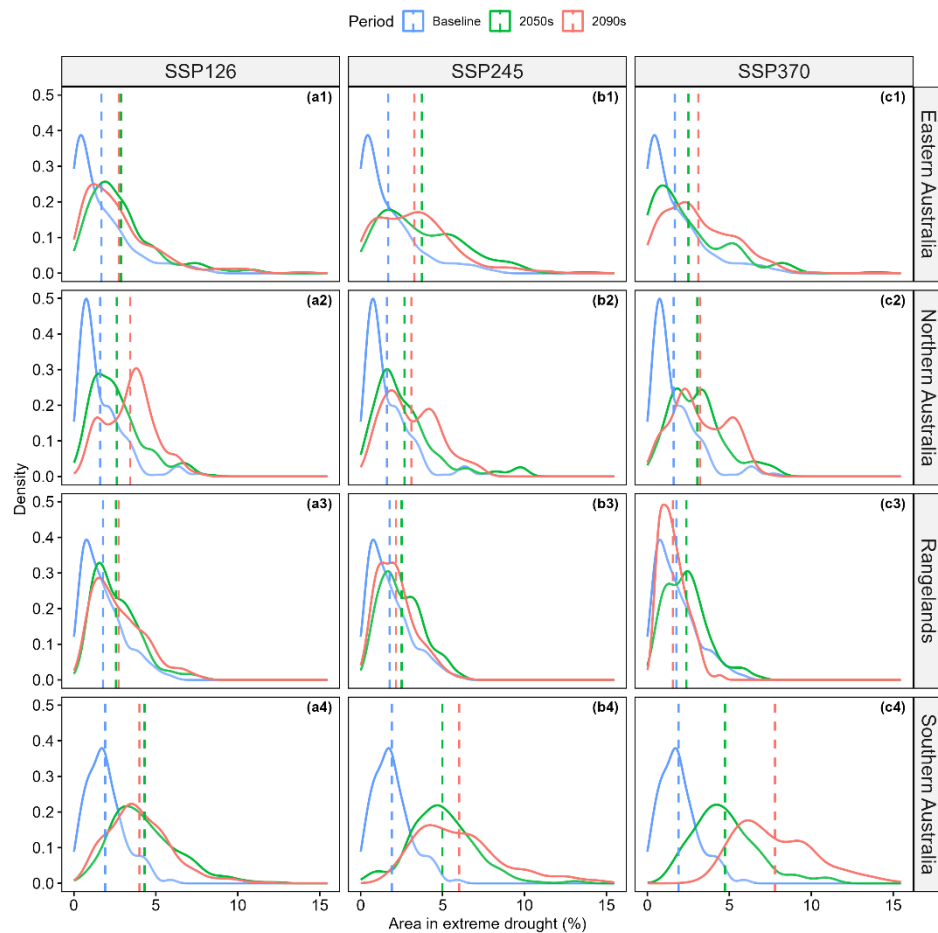
Figure 8: Probability density function plot the percent area under extreme drought using SPI-12 values from the ensemble average for the reference period (1995-2014), 2050s (2041-2060), and 2090s (2081-2100). Results are shown for the three SSPs in the four NRM super-clusters considered. Dotted lines show mean values.

320
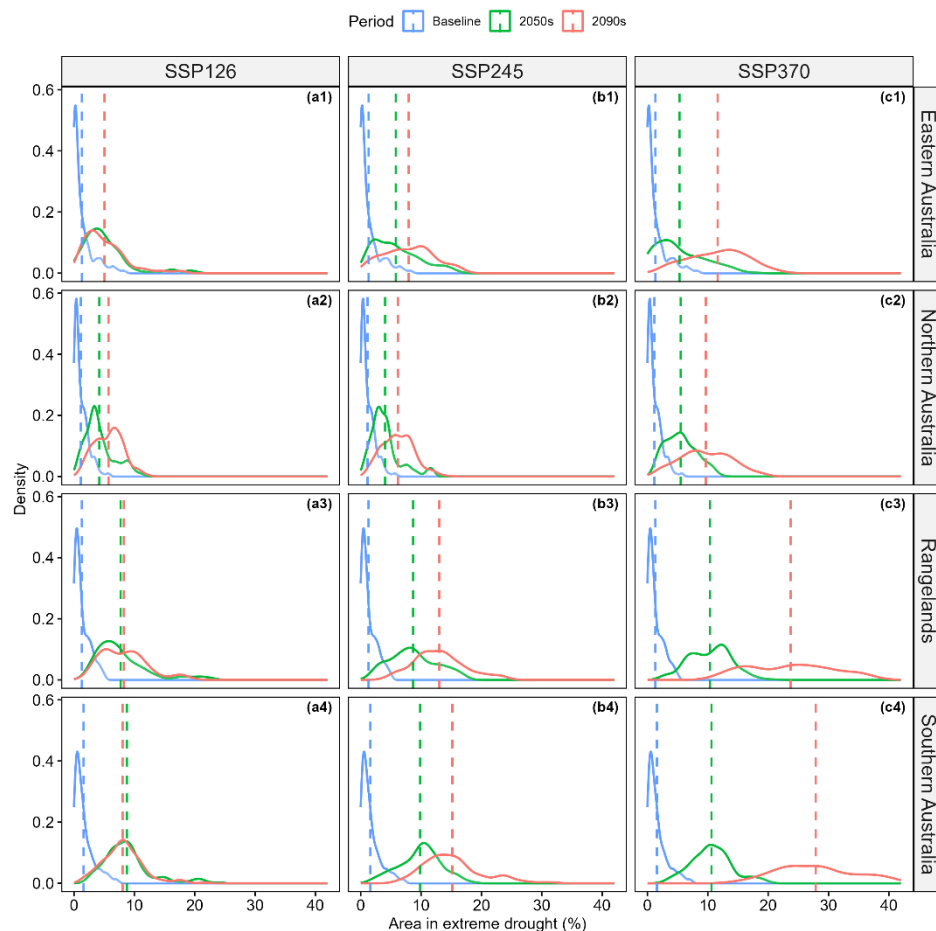
Figure 9: Probability density function plot the percent area under extreme drought using SPEI-12 values from the ensemble average for the reference period (1995-2014), 2050s (2041-2060), and 2090s (2081-2100). Results are shown for the three SSPs in the four NRM super-clusters considered. Dotted lines show mean values.

325

3.2.3 Changes to Drought Occurrence

There was wide model agreement on increased percent time in drought, frequency, and duration of droughts in south-west Western Australia, in southern Victoria, southern South Australia and in western Tasmania (Fig. 10) using both SPI and SPEI. In southwest Western Australia, SPI extreme droughts were projected to occur both more frequently and last longer, leading 330 to considerable increases in the percent time in drought. By contrast, the increases to the percent time in drought in southern Victoria, southern South Australia and in western Tasmania appears to be principally the result of increased drought frequency, with less clear changes noted for drought duration. In addition to these regions, there was also wide model agreement on increased frequency and percent time in moderate to extreme drought for the Gulf of Carpentaria and Northeastern Queensland

(Fig. S16), which was not evident in the extreme droughts. For the remainder of the country, the results of SPI tended to be
335 uncertain, though increases to the percent time in drought were seen for Eastern Australia under some emissions scenarios
(SSP245). Interestingly, there were no regions of Australia where there was a consensus towards reduced time in extreme
drought.

For SPEI, there was wide model agreement for more frequent and longer drought events for the majority of the continent,
particularly under SSP370 and for the end of the century (Fig. 10). This was especially true for the percentage time in drought,
340 which is the result of both increasing drought frequency and duration. For parts of Northern Australia and Eastern Australia,
there was generally less model agreement (as shown by the hatching) and the magnitude of the changes were typically smaller
when compared to southern regions and the interior of the continent.
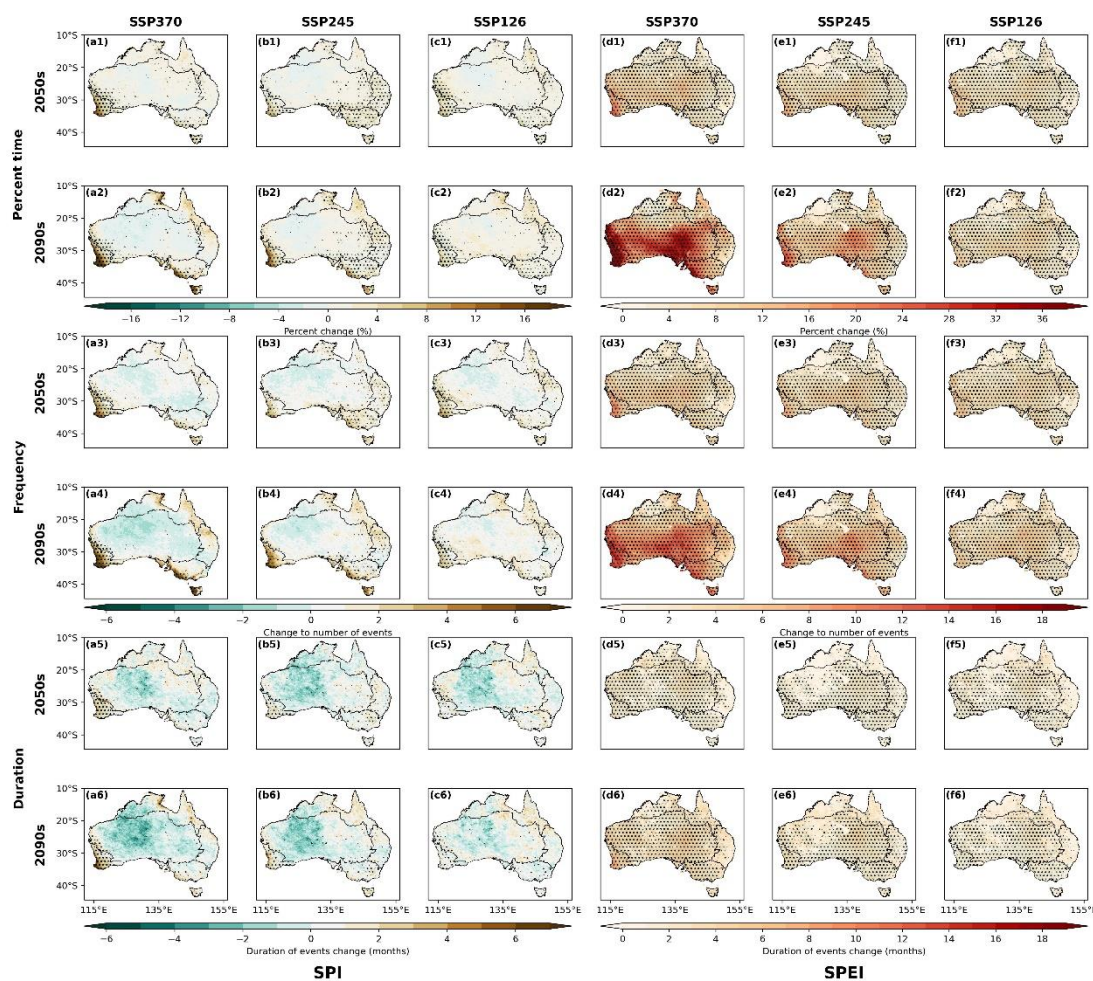
345 **Figure 10: Maps showing changes to the percent time (rows 1 to 2), frequency (rows 3 to 4), and duration (rows 5 to 6) of extreme droughts according to SPI (columns a, b, and c) and SPEI (column d, e, and f) for the 2050s and 2090s relative to the reference period. Hatching used where there was high inter-model agreement on the sign of change (>70%).**

Considerable inter-model variability was evident in the projections as shown by boxplots from the model ensemble (Fig. 11),
350   especially for SPEI. The variability was largest for the percent time in drought and frequency of droughts in the more arid
regions of Southern Australia and Rangelands. While for drought duration, the model variability was greater in the more humid
regions of Northern and Eastern Australia. When using SPEI there was very wide agreement towards more frequent and longer
extreme droughts from the full ensemble of models in all regions. For SPI there was less certainty on the sign of change in
most regions, except for Southern Australia where there was a clear tendency towards more frequent and longer extreme
355   droughts. For Southern Australia, there was agreement between SPI and SPEI on the sign of the change but not the magnitude.
For the other regions, the results were less certain, though generally most models appeared to point towards more frequent
extreme droughts, with an overall increase to the time spent in extreme droughts for all regions and emissions scenarios.
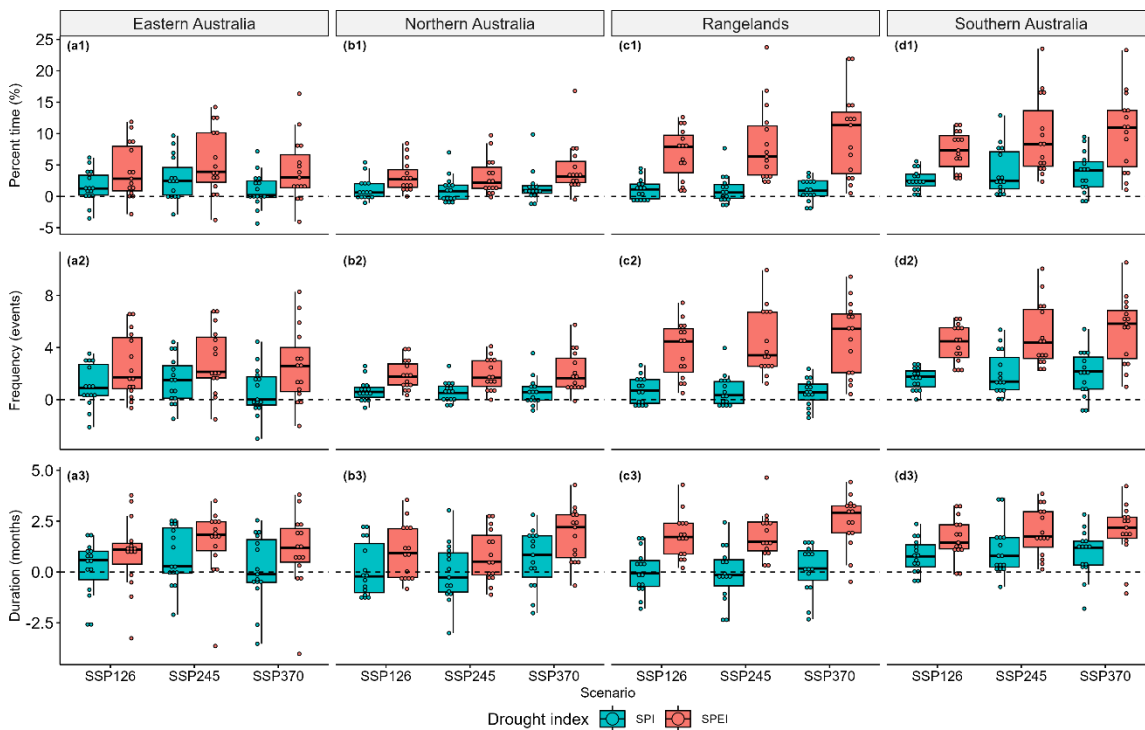
360   **Figure 11: Changes to the percent time, frequency, and duration of extreme droughts using SPI and SPEI in the 2050s compared to
the reference period. The box and whisker plot shows the interquartile range (box), and the median (bar), while the whiskers extend
from the box to the furthest datapoint within 1.5x the interquartile range. Dots show projections for each of the climate models.**

4 Discussion

4.1 Future Drought

365

Our study shows there is likely to be an increase in the frequency of droughts, particularly extreme droughts, across Australia, especially in Southern Australia and when assessing SPEI derived drought metrics. The results for SPI were more uncertain, reflecting uncertainty in rainfall projections. Both drought indices projected an increase to the time in, spatial extent, frequency, and duration of droughts in southwest Western Australia, southern South Australia, southern Victoria, and in western

370 Tasmania, especially by the end of the century and under high emissions (Fig. 10). These results are consistent with recent observations which have pointed towards a trend of decreasing precipitation for these regions (Dey et al., 2019), and are also consistent with recent global and regional assessments of future droughts (Cook et al., 2020; Herold et al., 2021; Kirono et al., 2020; Spinoni et al., 2020; Ukkola et al., 2020; Wang et al., 2021; Zeng et al., 2022). Using earlier CMIP5 projections, Kirono et al. (2020) showed a marked increase for future droughts in Southern Australia, which is in line with the findings from this

375 study. However, they also showed wide model agreement towards increased droughts in Eastern Australia using SPI, which was not reflected in this study to the same degree. This may relate to the selection of the climate model ensemble adopted, which has been shown to be one of the principal sources of uncertainty (Ukkola et al., 2018). Similarly, Trancoso et al. (2024) have shown that the precipitation agreement of the host GCMs is particularly low for Australia for both CMIP5 and CMIP6 models, except for the southwest Western Australia region.

380 Our results show considerable increases to the area affected by future extreme droughts, especially in Southern Australia and under the high emissions pathway. In the absence of strong mitigation of emissions (i.e. SSP370), an additional 5.9% increase to the area affected by extreme drought was expected using SPI in Southern Australia by the end of the century, which corresponds to a fourfold increase in the area affected compared to current conditions. Under a low emissions scenario (SSP126), these increases are reduced to 2.1% or a near doubling compared to current conditions (Fig. 8). Differences between

385 emission scenarios were greater when evaluating the results of SPEI. Here, we found cutting emissions from high to low levels by the end of the century would decrease the area affected by extreme droughts by a factor of 4 in Southern Australia, 3.2 in Rangelands, 1.9 in Northern Australia, and 2.8 in Eastern Australia (Fig. 9), highlighting the importance of meeting emission reduction targets. The increases to extreme droughts are larger than those projected for moderate droughts, particularly in Southern Australia and the Rangelands (Table 3). Extreme droughts have a disproportionate impact on agriculture, society,

390 and the environment compared to more moderate droughts (Noel et al., 2020; Potop, 2011), and as such these changes would likely necessitate robust adaptation measures. We provide supplementary datasets tailoring these projections to Australian river basins and local government areas are available from Eccles (2024), which may be useful for informing decisions on adaptation and drought preparedness.

Interestingly, the increase in extreme droughts did not lead to a decrease in extreme wetness, but rather mostly reduced time

395 in near normal climate conditions (Table 3). This was due to a shift in the mean and an overall flattening of the PDFs of SPI and SPEI as seen in Fig. 5 and Fig. 6, leading to more time in drought conditions. Similar PDFs changes have been noted in

global assessments of soil moisture, runoff, and the Palmer drought index under CMIP5 and CMIP6 (Zhao and Dai, 2015, 2022).

While there was wide model agreement on increased droughts for Southern Australia, our results point to less agreement
400   among the ensemble of climate models and between the two drought indices for the other regions assessed. The differences between the two drought indices were particularly notable, with SPEI tending towards increased droughts for the majority of the continent, while results from the precipitation-based SPI were more uncertain (Fig. 10). The differences between SPI and SPEI diverged further as the projections extended further into the future, with the largest differences noted by the end of the century and under the higher emissions scenario (Fig. 11), which corresponds to when atmospheric water demands from
405   elevated PET were largest. Similar differences between these indices have been noted in studies using CMIP6 GCMs (Wang et al., 2021; Zeng et al., 2022). This was also found to be the principal factor contributing to increased future soil moisture drought over Australia (Zhao and Dai, 2022). Divergences between these indices have also been observed in studies of the recent past, with the majority of the earth's landmass shown to have had a wetting trend using SPI between 1971 and 2022, and an opposing drying trend when evaluating SPEI (Nwayor and Robeson, 2023). For Australia, no trend was evident between
410   1980 and 2020 using SPI, while a significant drying was noted using SPEI (Vicente-Serrano et al., 2022).

4.2 Differences Between SPI and SPEI

Differences between SPI and SPEI were also more evident in arid and semi-arid regions such as the Rangelands, which receive relatively low precipitation but have high potential for evaporative loss. In these regions, proportional increases to PET projected under climate change are substantially greater than the magnitude of possible changes to precipitation. As such, the
415   relative impact of PET increases on the overall water budget (P – PET) is greater than in humid regions, where precipitation changes can be just as consequential. Precipitation variability has been shown to be the principal driver of SPEI in humid regions, while in arid regions PET is the principal driver (Vicente-Serrano et al., 2015). This is reflected in our projections of future drought for SPEI, with smaller projected increases and less model agreement evident in the more humid Northern and Eastern Australia compared to the Rangelands and Southern Australia (Fig. 10 and Fig. 11).

420   In this study, PET was derived using the Penman-Monteith method (Allen et al., 1998). This approach is more data intensive than simplified techniques that rely on temperature inputs only, but is considered more robust and has been recommended when data is available (Hosseinzadehtalaei et al., 2017; Sheffield et al., 2012). Purely temperature-based models such as Thornthwaite (Thornthwaite, 1948) and Hargreaves (Hargreaves and Samani, 1985) equations have been shown to overestimate future PET. A limitation of this approach is that the approach for deriving PET does not resolve interactions
425   between elevated CO_2 and vegetation (Trancoso et al., 2017). Specifically, studies have shown that elevated CO_2 results in reduced stomatal conductance and elevated water use efficiency of vegetation (Leakey et al., 2009), leading to reduced transpiration (Novick et al., 2016). However, increased fertilisation from elevated CO_2 would likely lead to increased leaf size (Pritchard et al., 1999) and increase transpiration.

While there is some disagreement on the magnitude of future PET increases, there is confidence in the sign of change, unlike
430 for precipitation for which there is much uncertainty around the sign of future changes (Trancoso et al., 2024). Under climate
change, increasing temperatures will lead to increased evaporative demand, impacting on the overall water budget. Studies
which adopt SPI only to assess future changes to droughts miss this important component and may therefore underestimate
future drought changes. On the other hand, there is potential that the SPEI could overestimates future drought magnitudes and
may better represent a conservative upper limit of potential future drought risk. Changes to other drought types may therefore
435 end up lying somewhere between these two indices, depending on the drought type and the region assessed (Reyniers et al.,
2023; Tomas-Burguera et al., 2020).

4.3 Implications

While this study focused only on meteorological droughts, these changes will have inevitable consequences for other drought
types (e.g. agricultural and hydrological), though it should be noted that the propagation from meteorological droughts to other
440 drought types is typically non-linear (Mukherjee et al., 2018). Significant decreasing trends for streamflow have been observed
for most of Australia in the recent past, with only catchments in the northern tropics showing an increasing trend
(Amirthanathan et al., 2023). This has led to increased hydrological droughts over much of southern Australia, which cannot
be explained by changes to rainfall alone (Wasko et al., 2021). In Southeast Australia, the Millenium drought (2001-2009) was
a major contributor to decreased streamflow (Fiddes and Timbal, 2016). However, despite the meteorological drought breaking
445 in 2010, a hydrological drought has persisted in many catchments, with runoff volumes significantly lower than pre-drought
conditions despite a return in precipitation (Fowler et al., 2022; Peterson et al., 2021). This suggests that hydrological droughts
can persist indefinitely following prolonged meteorological droughts (Peterson et al., 2021). Future increases to the time spent,
extent, and duration of meteorological droughts as suggested by this study may therefore have significant ramifications for
hydrological droughts in Australia, by effectively altering the long-term rainfall-runoff response. In southwest Western
450 Australia, observed streamflow declines have been attributed to a combination of decreased rainfall and increased vegetation
(Liu et al., 2019). CO_2 fertilisation may therefore work in tandem with meteorological droughts to further exacerbate future
hydrological droughts (Mankin et al., 2019; Trancoso et al., 2017) in spite of CO_2 induced changes to stomatal conductance
reducing plant transpiration changes.

Elevated PET during periods of precipitation deficit will likely increase the severity of plant stress due to differences between
455 the atmospheric water demand and the water available for transpiration (Anderegg et al., 2015). This can lead to plant dieback
and mortality, which may also be worsened from elevated heat stress due to a warming climate. Higher atmospheric water
demand can also work to dry out vegetation and elevate fire risk (Clarke et al., 2022). The recent tinderbox drought in southeast
Australia is an example of a drought characterised by below average rainfall, high atmospheric water demand, and reduced
water availability (Devanand et al., 2024). The high atmospheric water demand and limited water availability led to elevated
460 temperatures, amplified heatwaves, and likely contributed to the Black Summer bushfires (Devanand et al., 2024). An
amplification of future meteorological droughts characterised by elevated PET and higher temperatures may therefore lead to

an increase in such events, which will have obvious ramifications for bushfire risk and heatwaves. Further research is, however, required to quantify the magnitude of these future changes as a result of the projected meteorological drought changes.

5 Conclusion

465 We evaluated the impacts of climate change on meteorological droughts using two commonly adopted indices (SPI and SPEI). For this purpose, high-resolution CMIP6 climate models under three SSP scenarios were applied. The results show consistent increases in future frequency, duration, percent time, and spatial extent of SPI droughts for south-west Western Australia, southern Victoria, southern South Australia, and in western Tasmania, while a majority of Australia was projected to see increases according to SPEI. The increases were largest by the end of the century and under the high emission (SSP370)

470 scenario, especially for SPEI, as this is when increases to temperature and evaporative demand were greatest. There was greater certainty on the sign of change for droughts when assessing SPEI compared to SPI for all regions due to strong certainty of increasing PET, though there was still considerable uncertainty on the magnitude of the changes. Under a scenario of high emissions, a 4-fold increase in the area affected by extreme drought was expected for Southern Australia by the end of the century, considering just changes to rainfall (SPI). When the additional impacts of evaporative losses from PET were

475 considered (SPEI), there was a 17-fold increase in the area impacted compared to current conditions. Under a low emissions scenario, these changes decreased to 2-fold for SPI and 5-fold for SPEI, highlighting the importance of mitigating emissions. The relative changes were less substantial for the other NRM region clusters assessed, except for the Rangelands for which significant increases were shown when evaluating SPEI by the end of the century but not for SPI. Overall, our findings show strong increases in meteorological droughts for the majority of Australia, particularly in the southern region, by the end of the

480 century, and under high emissions scenarios. These results have multi-sectoral implications with strong impact on water supply and agriculture and we encourage stakeholders to explore the supplementary datasets with tailored drought calculations for Australian LGAs and basins to support decision-making.

Data availability

Datasets of regionalised drought changes are freely available from (Eccles, 2024,

485 https://doi.org/10.6084/m9.figshare.26343823)

The downscaled CCAM data used in this study is being published via the CORDEX Australasia domain archive. The 20km data for the Australasian CORDEX domain is available from NCI (National Computational Infrastructure): https://dx.doi.org/10.25914/8fve1910. Selected 10 km resolution data is available from NCI for registered users.

Author Contribution

490   Rohan Eccles: Writing – Original draft preparation, Conceptualization, Methodology, Formal analysis, Ralph Trancoso: Conceptualization, Methodology, Writing - Review & Editing, Jozef Syktus: Conceptualization, Data Curation, Methodology Sarah Chapman: Writing - Review & Editing, Data Curation, Visualization, Nathan Toombs: Writing - Review & Editing, Data Curation, Hong Zhang: Writing - Review & Editing, Data Curation, Shaoxiu Ma: Writing - Review & Editing, Ryan McGloin: Writing - Review & Editing

Competing Interests

495

The authors declare that they have no conflict of interest.

Acknowledgements

We acknowledge support by Lindsay Brebber from Information and Digital Science Delivery of the Department of Environment and Science for support with high performance computing and data storage.

500   **References**

Allen, R. G., Pereira, L. S., Raes, D., and Smith, M.: Crop evapotranspiration-Guidelines for computing crop water requirements-FAO Irrigation and drainage paper 56, 1998.

Amirthanathan, G. E., Bari, M. A., Woldemeskel, F. M., Tuteja, N. K., and Feikema, P. M.: Regional significance of historical trends and step changes in Australian streamflow, Hydrology and Earth System Sciences, 27, 229–254, 505   https://doi.org/10.5194/hess-27-229-2023, 2023.

Anderegg, W. R. L., Schwalm, C., Biondi, F., Camarero, J. J., Koch, G., Litvak, M., Ogle, K., Shaw, J. D., Shevliakova, E., Williams, A. P., Wolf, A., Ziaco, E., and Pacala, S.: Pervasive drought legacies in forest ecosystems and their implications for carbon cycle models, Science, 349, 528–532, https://doi.org/10.1126/science.aab1833, 2015.

Beguería, S., Vicente-Serrano, S. M., and Beguería, M. S.: Package 'spei,' Calculation of the Standardised Precipitation-510   Evapotranspiration Index, CRAN [Package], 2017.

Boé, J. and Terray, L.: Land–sea contrast, soil-atmosphere and cloud-temperature interactions: interplays and roles in future summer European climate change, Clim Dyn, 42, 683–699, https://doi.org/10.1007/s00382-013-1868-8, 2014.

Chapman, S., Syktus, J., Trancoso, R., Thatcher, M., Toombs, N., Wong, K. K.-H., and Takbash, A.: Evaluation of Dynamically Downscaled CMIP6-CCAM Models Over Australia, Earth's Future, 11, e2023EF003548, 515   https://doi.org/10.1029/2023EF003548, 2023.

Clarke, H., Nolan, R. H., De Dios, V. R., Bradstock, R., Griebel, A., Khanal, S., and Boer, M. M.: Forest fire threatens global carbon sinks and population centres under rising atmospheric water demand, Nat Commun, 13, 7161, https://doi.org/10.1038/s41467-022-34966-3, 2022.

Cook, B. I., Mankin, J. S., and Anchukaitis, K. J.: Climate Change and Drought: From Past to Future, Current Climate Change
520 Reports, 4, 164–179, https://doi.org/10.1007/s40641-018-0093-2, 2018.

Cook, B. I., Mankin, J. S., Marvel, K., Williams, A. P., Smerdon, J. E., and Anchukaitis, K. J.: Twenty-First Century Drought
Projections in the CMIP6 Forcing Scenarios, Earth's Future, 8, e2019EF001461, https://doi.org/10.1029/2019EF001461,
2020.

Devanand, A., Falster, G. M., Gillett, Z. E., Hobeichi, S., Holgate, C. M., Jin, C., Mu, M., Parker, T., Rifai, S. W., Rome, K.
525 S., Stojanovic, M., Vogel, E., Abram, N. J., Abramowitz, G., Coats, S., Evans, J. P., Gallant, A. J. E., Pitman, A. J., Power, S.
B., Rauniyar, S. P., Taschetto, A. S., and Ukkola, A. M.: Australia's Tinderbox Drought: An extreme natural event likely
worsened by human-caused climate change, Science Advances, 10, eadj3460, https://doi.org/10.1126/sciadv.adj3460, 2024.

Dey, R., Lewis, S. C., Arblaster, J. M., and Abram, N. J.: A review of past and projected changes in Australia's rainfall, WIREs
Climate Change, 10, e577, https://doi.org/10.1002/wcc.577, 2019.

530 Eccles, R.: Meteorological drought projections for Australia from downscaled high-resolution CMIP6 climate simulations,
Figshare, Dataset, https://doi.org/10.6084/m9.figshare.26343823, 2024.

Evans, A., Jones, D., Smalley, R., and Lellyett, S.: An enhanced gridded rainfall analysis scheme for Australia, Australian
Bureau of Meteorology: Melbourne, VIC, Australia, 66, 55–67, 2020.

Feng, P., Liu, D. L., Wang, B., Waters, C., Zhang, M., and Yu, Q.: Projected changes in drought across the wheat belt of
535 southeastern Australia using a downscaled climate ensemble, International Journal of Climatology, 39, 1041–1053,
https://doi.org/10.1002/joc.5861, 2019.

Fiddes, S. and Timbal, B.: Assessment and reconstruction of catchment streamflow trends and variability in response to rainfall
across Victoria, Australia, Climate Research, 67, 43–60, https://doi.org/10.3354/cr01355, 2016.

Gao, X., Zhao, Q., Zhao, X., Wu, P., Pan, W., Gao, X., and Sun, M.: Temporal and spatial evolution of the standardized
540 precipitation evapotranspiration index (SPEI) in the Loess Plateau under climate change from 2001 to 2050, Science of The
Total Environment, 595, 191–200, https://doi.org/10.1016/j.scitotenv.2017.03.226, 2017.

González Tánago, I., Urquijo, J., Blauhut, V., Villarroya, F., and De Stefano, L.: Learning from experience: a systematic
review of assessments of vulnerability to drought, Nat Hazards, 80, 951–973, https://doi.org/10.1007/s11069-015-2006-1,
2016.

545 Grose, M. R., Syktus, J., Thatcher, M., Evans, J. P., Ji, F., Rafter, T., and Remenyi, T.: The role of topography on projected
rainfall change in mid-latitude mountain regions, Climate Dynamics, 53, 3675–3690, https://doi.org/10.1007/s00382-019-
04736-x, 2019.

Grose, M. R., Narsey, S., Delage, F. P., Dowdy, A. J., Bador, M., Boschat, G., Chung, C., Kajtar, J. B., Rauniyar, S., Freund,
M. B., Lyu, K., Rashid, H., Zhang, X., Wales, S., Trenham, C., Holbrook, N. J., Cowan, T., Alexander, L., Arblaster, J. M.,
550 and Power, S.: Insights From CMIP6 for Australia's Future Climate, Earth's Future, 8, e2019EF001469,
https://doi.org/10.1029/2019EF001469, 2020.

Hargreaves, G. H. and Samani, Z. A.: Reference crop evapotranspiration from temperature, Applied engineering in agriculture,
1, 96–99, 1985.

He, M., Russo, M., and Anderson, M.: Hydroclimatic Characteristics of the 2012–2015 California Drought from an Operational
555 Perspective, Climate, 5, 5, https://doi.org/10.3390/cli5010005, 2017.

Herold, N., Downes, S. M., Gross, M. H., Ji, F., Nishant, N., Macadam, I., Ridder, N. N., and Beyer, K.: Projected changes in the frequency of climate extremes over southeast Australia, Environmental Research Communications, 3, 011001, https://doi.org/10.1088/2515-7620/abe6b1, 2021.

560 Hoffmann, P., Katzfey, J. J., McGregor, J. L., and Thatcher, M.: Bias and variance correction of sea surface temperatures used for dynamical downscaling, Journal of Geophysical Research, 121, 12,877-12,890, https://doi.org/10.1002/2016JD025383, 2016.

Horridge, M., Madden, J., and Wittwer, G.: The impact of the 2002–2003 drought on Australia, Journal of Policy Modeling, 27, 285–308, https://doi.org/10.1016/j.jpolmod.2005.01.008, 2005.

Hosseinzadehtalaei, P., Tabari, H., and Willems, P.: Quantification of uncertainty in reference evapotranspiration climate
565 change signals in Belgium, Hydrology Research, 48, 1391–1401, https://doi.org/10.2166/nh.2016.243, 2017.

Huang, J., Yu, H., Guan, X., Wang, G., and Guo, R.: Accelerated dryland expansion under climate change, Nature Clim Change, 6, 166–171, https://doi.org/10.1038/nclimate2837, 2016.

IPCC: Climate Change 2021 – The Physical Science Basis: Working Group I Contribution to the Sixth Assessment Report of the Intergovernmental Panel on Climate Change, Cambridge University Press, Cambridge,
570 https://doi.org/10.1017/9781009157896, 2023.

Johnston, F., Hanigan, I., Henderson, S., Morgan, G., and Bowman, D.: Extreme air pollution events from bushfires and dust storms and their association with mortality in Sydney, Australia 1994–2007, Environmental Research, 111, 811–816, https://doi.org/10.1016/j.envres.2011.05.007, 2011.

Kelley, C. P., Mohtadi, S., Cane, M. A., Seager, R., and Kushnir, Y.: Climate change in the Fertile Crescent and implications
575 of the recent Syrian drought, Proceedings of the National Academy of Sciences, 112, 3241–3246, https://doi.org/10.1073/pnas.1421533112, 2015.

Kiem, A. S., Johnson, F., Westra, S., van Dijk, A., Evans, J. P., O'Donnell, A., Rouillard, A., Barr, C., Tyler, J., Thyer, M., Jakob, D., Woldemeskel, F., Sivakumar, B., and Mehrotra, R.: Natural hazards in Australia: droughts, Climatic Change, 139, 37–54, https://doi.org/10.1007/s10584-016-1798-7, 2016.

580 Kim, Y., Rocheta, E., Evans, J. P., and Sharma, A.: Impact of bias correction of regional climate model boundary conditions on the simulation of precipitation extremes, Climate Dynamics, 55, 3507–3526, https://doi.org/10.1007/S00382-020-05462-5/FIGURES/10, 2020.

Kirono, D. G. C. and Kent, D. M.: Assessment of rainfall and potential evaporation from global climate models and its implications for Australian regional drought projection, International Journal of Climatology, 31, 1295–1308,
585 https://doi.org/10.1002/joc.2165, 2011.

Kirono, D. G. C., Kent, D. M., Hennessy, K. J., and Mpelasoka, F.: Characteristics of Australian droughts under enhanced greenhouse conditions: Results from 14 global climate models, Journal of Arid Environments, 75, 566–575, https://doi.org/10.1016/j.jaridenv.2010.12.012, 2011.

Kirono, D. G. C., Round, V., Heady, C., Chiew, F. H. S., and Osbrough, S.: Drought projections for Australia: Updated results
590 and analysis of model simulations, Weather and Climate Extremes, 30, 100280, https://doi.org/10.1016/j.wace.2020.100280, 2020.

Labudová, L., Labuda, M., and Takáč, J.: Comparison of SPI and SPEI applicability for drought impact assessment on crop production in the Danubian Lowland and the East Slovakian Lowland, Theoretical and Applied Climatology, 128, 491–506, https://doi.org/10.1007/s00704-016-1870-2, 2017.

595   Leakey, A. D. B., Ainsworth, E. A., Bernacchi, C. J., Rogers, A., Long, S. P., and Ort, D. R.: Elevated CO2 effects on plant carbon, nitrogen, and water relations: six important lessons from FACE, J Exp Bot, 60, 2859–2876, https://doi.org/10.1093/jxb/erp096, 2009.

Leys, J., Heidenreich, S., White, S., Guerschman, J., and Strong, C.: Dust-storm frequencies, community attitudes, government policy and land management practices during three major droughts in New South Wales, Australia, Rangel. J.,
600   https://doi.org/10.1071/RJ22059, 2023.

Lim, C. M., Yhang, Y. B., and Ham, S.: Application of GCM Bias Correction to RCM Simulations of East Asian Winter Climate, Atmosphere 2019, Vol. 10, Page 382, 10, 382, https://doi.org/10.3390/ATMOS10070382, 2019.

Liu, N., Harper, R. J., Smettem, K. R. J., Dell, B., and Liu, S.: Responses of streamflow to vegetation and climate change in southwestern Australia, Journal of Hydrology, 572, 761–770, https://doi.org/10.1016/j.jhydrol.2019.03.005, 2019.

605   Maier, H. R., Paton, F. L., Dandy, G. C., and Connor, J. D.: Impact of Drought on Adelaide's Water Supply System: Past, Present, and Future, in: Drought in Arid and Semi-Arid Regions: A Multi-Disciplinary and Cross-Country Perspective, edited by: Schwabe, K., Albiac, J., Connor, J. D., Hassan, R. M., and Meza González, L., Springer Netherlands, Dordrecht, 41–62, https://doi.org/10.1007/978-94-007-6636-5_3, 2013.

Mankin, J. S., Seager, R., Smerdon, J. E., Cook, B. I., and Williams, A. P.: Mid-latitude freshwater availability reduced by
610   projected vegetation responses to climate change, Nat. Geosci., 12, 983–988, https://doi.org/10.1038/s41561-019-0480-x, 2019.

McGregor, J. L. and Dix, M. R.: An updated description of the conformal-cubic atmospheric model, in: High Resolution Numerical Modelling of the Atmosphere and Ocean, Springer New York, 51–75, 2008.

McKee, T. B., Doesken, N. J., and Kleist, J.: The Relationship of Drought Frequency and Duration to Time Scales, in:
615   Proceedings of the 8th Conference on Applied Climatology., 1993.

Mpelasoka, F., Hennessy, K., Jones, R., and Bates, B.: Comparison of suitable drought indices for climate change impacts assessment over Australia towards resource management, Int. J. Climatol., 28, 1283–1292, https://doi.org/10.1002/joc.1649, 2008.

Mukherjee, S., Mishra, A., and Trenberth, K. E.: Climate Change and Drought: a Perspective on Drought Indices, Curr Clim
620   Change Rep, 4, 145–163, https://doi.org/10.1007/s40641-018-0098-x, 2018.

Noel, M., Bathke, D., Fuchs, B., Gutzmer, D., Haigh, T., Hayes, M., Poděbradská, M., Shield, C., Smith, K., and Svoboda, M.: Linking Drought Impacts to Drought Severity at the State Level, https://doi.org/10.1175/BAMS-D-19-0067.1, 2020.

Novick, K. A., Ficklin, D. L., Stoy, P. C., Williams, C. A., Bohrer, G., Oishi, A. C., Papuga, S. A., Blanken, P. D., Noormets, A., Sulman, B. N., Scott, R. L., Wang, L., and Phillips, R. P.: The increasing importance of atmospheric demand for ecosystem
625   water and carbon fluxes, Nature Clim Change, 6, 1023–1027, https://doi.org/10.1038/nclimate3114, 2016.

Nwayor, I. J. and Robeson, S. M.: Exploring the relationship between SPI and SPEI in a warming world, Theor Appl Climatol, https://doi.org/10.1007/s00704-023-04764-y, 2023.

Peterson, T. J., Saft, M., Peel, M. C., and John, A.: Watersheds may not recover from drought, Science, 372, 745–749, https://doi.org/10.1126/science.abd5085, 2021.

630 Potop, V.: Evolution of drought severity and its impact on corn in the Republic of Moldova, Theor Appl Climatol, 105, 469–483, https://doi.org/10.1007/s00704-011-0403-2, 2011.

Pritchard, SetH. G., Rogers, HugO. H., Prior, S. A., and Peterson, CurT. M.: Elevated CO2 and plant structure: a review, Global Change Biology, 5, 807–837, https://doi.org/10.1046/j.1365-2486.1999.00268.x, 1999.

Reder, A., Raffa, M., Montesarchio, M., and Mercogliano, P.: Performance evaluation of regional climate model simulations 635 at different spatial and temporal scales over the complex orography area of the Alpine region, Natural Hazards, 102, 151–177, https://doi.org/10.1007/S11069-020-03916-X/FIGURES/14, 2020.

Reyniers, N., Osborn, T. J., Addor, N., and Darch, G.: Projected changes in droughts and extreme droughts in Great Britain strongly influenced by the choice of drought index, Hydrology and Earth System Sciences, 27, 1151–1171, https://doi.org/10.5194/hess-27-1151-2023, 2023.

640 Secci, D., Tanda, M. G., D'Oria, M., Todaro, V., and Fagandini, C.: Impacts of climate change on groundwater droughts by means of standardized indices and regional climate models, Journal of Hydrology, 603, 127154, https://doi.org/10.1016/j.jhydrol.2021.127154, 2021.

Sheffield, J., Wood, E. F., and Roderick, M. L.: Little change in global drought over the past 60 years, Nature, 491, 435–438, https://doi.org/10.1038/nature11575, 2012.

645 Shi, L., Feng, P., Wang, B., Liu, D. L., and Yu, Q.: Quantifying future drought change and associated uncertainty in southeastern Australia with multiple potential evapotranspiration models, Journal of Hydrology, 590, 125394, https://doi.org/10.1016/j.jhydrol.2020.125394, 2020.

Spinoni, J., Vogt, J. V., Naumann, G., Barbosa, P., and Dosio, A.: Will drought events become more frequent and severe in Europe?: FUTURE DROUGHT EVENTS IN EUROPE, Int. J. Climatol, 38, 1718–1736, https://doi.org/10.1002/joc.5291, 650 2018.

Spinoni, J., Barbosa, P., Bucchignani, E., Cassano, J., Cavazos, T., Christensen, J. H., Christensen, O. B., Coppola, E., Evans, J., Geyer, B., Giorgi, F., Hadjinicolaou, P., Jacob, D., Katzfey, J., Koenigk, T., Laprise, R., Lennard, C. J., Kurnaz, M. L., Delei, L. I., Llopart, M., McCormick, N., Naumann, G., Nikulin, G., Ozturk, T., Panitz, H. J., da Rocha, R. P., Rockel, B., Solman, S. A., Syktus, J., Tangang, F., Teichmann, C., Vautard, R., Vogt, J. V., Winger, K., Zittis, G., and Dosio, A.: Future 655 Global Meteorological Drought Hot Spots: A Study Based on CORDEX Data, Journal of Climate, 33, 3635–3661, https://doi.org/10.1175/JCLI-D-19-0084.1, 2020.

Svoboda, M. and Fuchs, B. A.: Handbook of drought indicators and indices, World Meteorological Organization Geneva, Switzerland, 2016.

Svoboda, M., Hayes, M., and Wood, D.: Standardized precipitation index: user guide, 2012.

660 Syktus, J., Toombs, N., Wong, K., Trancoso, R., and Ahrens, D.: Queensland Future Climate Dataset – Downscaled CMIP5 climate projections for RCP8.5 and RCP4.5, , https://doi.org/10.25901/5e3ba30f141b7, 2020.

Scientific description - CCAM.: https://confluence.csiro.au/display/CCAM/Scientific+description.

Thornthwaite, C. W.: An approach toward a rational classification of climate, Geographical review, 38, 55–94, 1948.

Tian, T., Boberg, F., Christensen, O. B., Christensen, J. H., She, J., and Vihma, T.: Resolved complex coastlines and land–sea
665   contrasts in a high-resolution regional climate model: a comparative study using prescribed and modelled SSTs, Tellus A:
Dynamic Meteorology and Oceanography, 65, 19951, https://doi.org/10.3402/tellusa.v65i0.19951, 2013.

Tomas-Burguera, M., Vicente-Serrano, S. M., Peña-Angulo, D., Domínguez-Castro, F., Noguera, I., and El Kenawy, A.:
Global Characterization of the Varying Responses of the Standardized Precipitation Evapotranspiration Index to Atmospheric
Evaporative Demand, Journal of Geophysical Research: Atmospheres, 125, e2020JD033017,
670   https://doi.org/10.1029/2020JD033017, 2020.

Trancoso, R., Larsen, J., McVicar, T., Phinn, S., and Mcalpine, C.: CO2 – vegetation feedbacks and other climate changes
implicated in reducing baseflow, Geophysical Research Letters, 44, https://doi.org/10.1002/2017GL072759, 2017.

Trancoso, R., Syktus, J., Toombs, N., and Chapman, S.: Assessing and selecting CMIP6 GCMs ensemble runs based on their
ability to represent historical climate and future climate change signal, Copernicus Meetings,
675   https://doi.org/10.5194/egusphere-egu23-11412, 2023.

Trancoso, R., Syktus, J., Allan, R. P., Croke, J., Hoegh-Guldberg, O., and Chadwick, R.: Significantly wetter or drier future
conditions for one to two thirds of the world's population, Nat Commun, 15, 483, https://doi.org/10.1038/s41467-023-44513-
3, 2024.

Ukkola, A., Pitman, A., De Kauwe, M., Abramowitz, G., Herger, N., Evans, J., and Decker, M.: Evaluating CMIP5 model
680   agreement for multiple drought metrics, Journal of Hydrometeorology, 19, 969–988, 2018.

Ukkola, A., De Kauwe, M. G., Roderick, M. L., Abramowitz, G., and Pitman, A. J.: Robust future changes in meteorological
drought in CMIP6 projections despite uncertainty in precipitation, Geophysical Research Letters, 47, e2020GL087820, 2020.

United Nations Office for Disaster Risk Reduction and Centre for Research on the Epidemiology of Disasters: Economic
Losses, Poverty, & Disasters 1998-2017, 2018.

685   Van Dijk, A. I. J. M., Beck, H. E., Crosbie, R. S., De Jeu, R. A. M., Liu, Y. Y., Podger, G. M., Timbal, B., and Viney, N. R.:
The Millennium Drought in southeast Australia (2001-2009): Natural and human causes and implications for water resources,
ecosystems, economy, and society, Water Resources Research, 49, 1040–1057, https://doi.org/10.1002/wrcr.20123, 2013.

Vicente-Serrano, S. M., Beguería, S., and López-Moreno, J. I.: A multiscalar drought index sensitive to global warming: The
standardized precipitation evapotranspiration index, Journal of Climate, 23, 1696–1718,
690   https://doi.org/10.1175/2009JCLI2909.1, 2010.

Vicente-Serrano, S. M., Van der Schrier, G., Beguería, S., Azorin-Molina, C., and Lopez-Moreno, J.-I.: Contribution of
precipitation and reference evapotranspiration to drought indices under different climates, Journal of Hydrology, 526, 42–54,
https://doi.org/10.1016/j.jhydrol.2014.11.025, 2015.

Vicente-Serrano, S. M., Peña-Angulo, D., Beguería, S., Domínguez-Castro, F., Tomás-Burguera, M., Noguera, I., Gimeno-
695   Sotelo, L., and El Kenawy, A.: Global drought trends and future projections, Philosophical Transactions of the Royal Society
A: Mathematical, Physical and Engineering Sciences, 380, 20210285, https://doi.org/10.1098/rsta.2021.0285, 2022.

Wang, T., Tu, X., Singh, V. P., Chen, X., and Lin, K.: Global data assessment and analysis of drought characteristics based on
CMIP6, Journal of Hydrology, 596, 126091, https://doi.org/10.1016/j.jhydrol.2021.126091, 2021.

Wasko, C., Shao, Y., Vogel, E., Wilson, L., Wang, Q. J., Frost, A., and Donnelly, C.: Understanding trends in hydrologic
700   extremes across Australia, Journal of Hydrology, 593, 125877, https://doi.org/10.1016/j.jhydrol.2020.125877, 2021.

Xiang, K., Wang, B., Liu, D. L., Chen, C., Waters, C., Huete, A., and Yu, Q.: Probabilistic assessment of drought impacts on wheat yield in south-eastern Australia, Agricultural Water Management, 284, 108359, https://doi.org/10.1016/j.agwat.2023.108359, 2023.

705   Zargar, A., Sadiq, R., Naser, B., and Khan, F. I.: A review of drought indices, Environ. Rev., 19, 333–349, https://doi.org/10.1139/a11-013, 2011.

Zeng, J., Li, J., Lu, X., Wei, Z., Shangguan, W., Zhang, S., Dai, Y., and Zhang, S.: Assessment of global meteorological, hydrological and agricultural drought under future warming based on CMIP6, Atmospheric and Oceanic Science Letters, 15, 100143, https://doi.org/10.1016/j.aosl.2021.100143, 2022.

Zhao, T. and Dai, A.: The Magnitude and Causes of Global Drought Changes in the Twenty-First Century under a Low–
710   Moderate Emissions Scenario, Journal of Climate, 28, 4490–4512, https://doi.org/10.1175/JCLI-D-14-00363.1, 2015.

Zhao, T. and Dai, A.: CMIP6 Model-Projected Hydroclimatic and Drought Changes and Their Causes in the Twenty-First Century, Journal of Climate, 35, 897–921, https://doi.org/10.1175/JCLI-D-21-0442.1, 2022.